Exploring the family feud: a fungal endophyte induces local cell wall-mediated resistance in wheat roots against the closely related "take-all" pathogen

Tania Chancellor[1,2], Daniel P. Smith[1], Wanxin Chen[1], Suzanne J. Clark[1], Eudri Venter[1,3], Kirstie Halsey[1], Vanessa McMillan[1,4], Gail Canning[1], Kim E. Hammond-Kosack[1], Javier Palma-Guerrero[1,5]

Affiliations:

[1]Rothamsted Research, Strategic Areas: Protecting Crops and the Environment, Intelligent Data Ecosystems, Plant Sciences for the Bioeconomy, West Common, Harpenden, AL5 2JQ, UK. [2] Crop Science Centre, Department of Plant Sciences, University of Cambridge, 93 Lawrence Weaver Road, Cambridge CB3 0LE, UK. [3] JEOL (UK) Ltd. JEOL House, Silver Court, Watchmead, Welwyn Garden City, Hertfordshire, AL7 1LT. [4] NIAB, 93 Lawrence Weaver Road, Cambridge CB3 0LE, UK. [5] FIBL Research Institute of Organic Agriculture, Ackerstrasse 113, 5070 Frick, Switzerland.

Correspondence: javier.palma@fibl.org (JPG), kim.hammond-kosack@rothamsted.ac.uk (KHK), tjc81@cam.ac.uk (TC)

ORCID IDs: 0000-0002-0867-7601 (JPG), 0000-0002-9699-485X (KHK), 0000-0002-3407-1697 (TC)

Abstract

Take-all disease, caused by the soil-borne ascomycete fungus *Gaeumannomyces tritici*, is one of the most important root diseases of wheat in the UK and worldwide. The fungus invades the roots and destroys the vascular tissue, hindering the uptake of water and nutrients from the soil. Closely related non-pathogenic species in the *Magnaporthaceae* family, such as *Gaeumannomyces hyphopodioides*, occur naturally in arable and grassland soils and have previously been reported to reduce take-all disease in field studies. Here, we characterise the different infection structures produced by *G. tritici* and *G. hyphopodioides* and suggest an alternative role for previously described "sub-epidermal vesicles" (SEVs). We show that direct interaction between the two species is unlikely to play a significant role in take-all control, and instead demonstrate that take-all control is achieved via local host changes in response to prior *G. hyphopodioides* root colonisation. RNA sequencing revealed extensive host transcriptional reprogramming in *G. hyphopodioides* colonised tissues, characterised by a striking downregulation of key cell-wall related genes, including cellulose synthase (CESA), and xyloglucan endotransglucosylase/hydrolase (XTH) genes. In the absence of take-all resistant wheat cultivars and avirulent *G. tritici* strains, studying closely related *G. hyphopodioides* provides a much-needed avenue to elucidate take-all resistance mechanisms in wheat.

Keywords: wheat root transcriptomes, endophyte, root pathogen, host defences, cell wall, biocontrol

Introduction

Wheat (*Triticum aestivum*) is considered one of the most important cereal crops worldwide, providing around 20% of human caloric intake globally. Sustaining good root health is critical for the acquisition of water and essential nutrients. As global temperatures continue to rise,

root health is predicted to face increasing threats from a growing number of potential soil-borne fungal pathogens which could jeopardise future food production (Delgado-Baquerizo et al., 2020). The necrotrophic fungal pathogen *Gaeumannomyces tritici*, belonging to the *Magnaporthaceae* family, is responsible for one of the most important root diseases of wheat worldwide (Freeman & Ward, 2004; Palma-Guerrero et al., 2021). The disease is commonly known as “take-all”, owing to the pathogen’s ability to drastically diminish grain yields during heavy infection episodes. However, due to the genetic intractability of *G. tritici*, both the pathogen and the cereal-pathosystem remain understudied in the molecular plant-microbe interaction (MPMI) community (Palma-Guerrero et al., 2021). Vascular infection by *G. tritici* results in the development of characteristic necrotic lesions originating from the root stele which severely disrupt water and nutrient uptake, causing early ripening of the crop, reduced grain yield and quality (Asher & Shipton, 1981; Huang et al., 2001). Take-all inoculum builds up in the soil following consecutive wheat crops, and though recent surveys of take-all disease levels are lacking, yield losses of up to 60% have been reported in the UK (McMillan et al., 2011). At present, take-all resistant wheat cultivars are not commercially available, and current fungicide seed treatments do not provide complete protection (Freeman et al., 2005).

Understanding root immunity is essential for the development of take-all resistant cultivars. However, the classical model of immunity, characterised by the concerted effect of pathogen-associated molecular pattern (PAMP) triggered immune responses (PTI) and effector triggered immune responses (ETI), is largely based on foliar pathogens (Boller & Felix, 2009; Jones & Dangl, 2006; Pok et al., 2022). Roots must constantly interact with a diverse soil microbiome and distinguish pathogenic microbes from, sometimes closely related, non-pathogenic endophytes or beneficial symbionts (Thoms et al., 2021). How plants engage with beneficial microorganisms while restricting damaging pathogens is regarded as one of the top 10 unanswered questions by the molecular plant microbe-interaction (MPMI) research community (Harris et al., 2020). The selective response of plants to microbes with different lifestyles can be partly explained by the compartmentalisation of localised immune responses in roots (Zhou et al., 2020), and the recognition of microbe-associated molecular patterns (MAMPs), damage-associated molecular patterns (DAMPs) and PAMPs by multiple receptors (Thoms et al., 2021). However, further comparative studies into endophytic and pathogenic plant infecting microbes are sorely needed.

Several members of the *Magnaporthaceae* family were previously classified within the Gaeumannomyces-Phialophora complex, which formerly consisted of the *Gaeumannomyces* fungi and their non-pathogenic asexual anamorphs, the *Phialophora* fungi (Hernández-Restrepo et al., 2016). *Phialophora* species, such as *Gaeumannomyces hyphopodioides,* occur naturally in grasslands and arable field sites, though do not cause disease symptoms in arable crops (Deacon, 1973; Ulrich et al., 2000; Ward & Bateman, 1999). For this reason, such species have been described as “non-pathogenic”. Prior colonisation by certain non-pathogenic *Magnaporthaceae* species is reported to provide protection against take-all disease in field studies (Wong et al., 1996). Some elite winter wheat varieties have an improved ability to promote *G. hyphopodioides* in field soils (Osborne et al., 2018), making the species a promising candidate for biocontrol.

The existence of endophytic species conferring resistance against closely related pathogens is not limited to the *Magnaporthaceae* family. Non-pathogenic strains in the *Fusarium oxysporum* species complex are known to provide protection against Fusarium wilt disease, a major disease caused by pathogenic *F. oxysporum* strains (de Lamo & Takken, 2020). This phenomenon, termed endophyte-mediated resistance (EMR), is reportedly independent of jasmonic acid (JA), ethylene (ET) and salicylic acid (SA) signalling (Constantin et al., 2019). However, the specific mechanisms mediating *G. hyphopodioides*-induced disease control are unknown and, as far as we are aware, the transcriptional responses of wheat to colonisation by *G. hyphopodioides* have not previously been investigated. Here, we provide the first comparative analysis of wheat transcriptional responses to *G. tritici* and *G. hyphopodioides* across key stages of early fungal infection, and characterise the different fungal structures

produced during root infection. Our findings shed light on the distinct plant responses to two closely related root infecting fungi with contrasting lifestyles, elucidating mechanisms for the control of take-all disease by *G. hyphopodioides*. Together, our findings contribute to an improved understanding of wheat root resistance against take-all disease.

Materials and Methods

Fungal isolation and culture

G. hyphopodioides (taxon id: 1940676) and *G. tritici* (taxon id: 36779) strains were isolated from field soils at Rothamsted Farm using the soil baiting method (McMillan et al., 2011; Osborne et al., 2018). Fungal isolates were maintained on potato dextrose agar (PDA) plates at 21°C in the dark (see table 1). Genetic typing of *G. tritici* isolates was carried out following the method described by (Freeman et al., 2005).

Table 1. Fungal isolates used in the present study.

Isolate	Rothamsted field name	Year isolated	Plot species, cultivar	ITS species identification	*G. tritici* genetic "type"
NZ.129.2C.17	New Zealand	2016	*T. aestivum*, Scout	*G. hyphopodioides*	-
105C-2	Delafield	2018	*T. aestivum*, Cadenza	Unnamed *Magnaporthaceae* sp.	-
H23-SB-2B	Highfield	2018	Grassland, Soft Brome (*Bromus hordeaceus*)	*Slopeiomyces cylindrosporus*	-
16.NZ.1d	New Zealand	2016	*T. aestivum*, Hereford	*G. tritici*	A
17LH(4)19d1	Long Hoos	2017	*T. aestivum*, Cadenza	*G. tritici*	A

Seedling pot infection assays and disease quantifications

For root inoculation experiments, plastic pots (7.5 cm wide x 11 cm tall) were filled with damp horticultural sand and ten wheat seeds (cv. Hereward) were sown on the surface. Seeds were covered with a thin layer of grit and pots were placed in a controlled environment growth room for two weeks (16 hr day, light intensity 250 µmols, 15 °C day, 10 °C night). *G. tritici* (isolate 16.NZ.1d) and *G. hyphopodioides* (isolate NZ.129.2C.17) inoculum was prepared by placing ten fungal plugs (7 mm diameter) taken from the leading edge of each colony into a 1 L flask containing 400 ml potato dextrose broth (PDB). Flasks were placed in an orbital incubator for 7 days at 25 °C, 120 RPM. Liquid cultures were homogenised and diluted with sterile distilled water in a 2:3 ratio. The first inoculum treatment was added into the pots after two weeks of plant growth. Inoculum (50 ml) was poured directly onto the root system using a funnel inserted into the sand. Five replicates were prepared per treatment, and the experiment was repeated twice.

For split-root experiments, roots from five 2-week old wheat seedlings (cv. Chinese Spring) were arranged in split-root chambers filled with sand and covered with grit, as above. Plants were immediately inoculated with *G. hyphopodioides* (isolate NZ.129.2C.17) as above, followed by *G. tritici* (isolate 17LH(4)19d1) one week later. Five replicates were prepared per treatment, and the experiment was repeated three times.

All seedlings were harvested three weeks after the final inoculum addition to allow take-all disease symptoms to develop. Visual disease assessments were carried out as previously

described (McMillan et al., 2011) and qPCR quantification of *G. tritici* fungal biomass was performed by targeting a 105-bp partial DNA sequence of the translation elongation factor 1-alpha (EF1-α) gene, using primers GtEFF1 (5'-CCCTGCAAGCTCTTCCTCTTAG-3') and GtEFR1 (5'-GCATGCGAGGTCCCAAAA-3') with the TaqMan probe (5'-6FAM-ACTGCACAGACCATC-MGB-3') (Thermo Scientific™, USA) (Keenan et al., 2015).

Plant growth, inoculation and root sampling for RNA sequencing and bioimaging

A precision inoculation method was developed to enable the investigation of local plant responses to fungal infection. Wheat seeds cv. Chinese Spring were surface sterilised with 5% (v/v) sodium hypochlorite for five minutes and pre-germinated in a controlled environment growth chamber cabinet (20 °C day, 16 °C night, 16 hr light cycle) for two days. Three pre-germinated seeds were transplanted onto a square petri dish plate (12 cm x 12 cm) containing 1.5 % (w/v) water agar. Five replicates were prepared for each treatment. Plates were placed horizontally in the growth cabinet. After four days, one root from each plant was inoculated with a fungal plug (4 cm x 0.5 cm) cut from the leading edge of a fungal colony growing on 1.5 % water agar. Inoculated roots were sampled daily from 2-6 days post inoculation (dpi). Briefly, two 1 cm root samples were harvested from the inoculated area on each root and snap frozen in liquid nitrogen for RNA extraction. To determine the stage of fungal colonisation in these harvested samples, 2 cm x 0.5 cm root pieces were sampled from the areas directly above and below each sample (see figure S1). Root pieces were stored in 50% ethanol for subsequent assessment by confocal microscopy.

Microscopy

Transmission electron microscopy of *G. hyphopodioides* sub-epidermal vesicles (SEVs)

Root pieces containing mature *G. hyphopodioides* SEVs were harvested from a seedling pot infection assay (see above). Samples were prepared for transmission electron microscopy (TEM) analysis by high-pressure freezing (Leica HPM100), followed by freeze substitution with ethanol (Leica EM AFS2) and infiltration with LR White resin (Agar Scientific). Ultrathin sections (90 nm thickness) were cut using a UC7 Ultramicrotome (Leica Microsystems). Due to the large size of *G. hyphopodioides* SEVs, a subset of semi-thin sections were stained and analysed by light microscopy to allow visualisation of entire SEVs (see below).

The remaining ultrathin sections were collected onto copper grids and stained with 2.5% uranyl acetate and Reynolds lead citrate (Reynolds, 1963). Ultrathin sections were imaged using a JEOL-2100 Plus Transmission Electron Microscope (JEOL, Japan) equipped with a Gatan OneView IS Camera (Gatan, USA). ImageJ software (https://imagej.net/) was used to measure the cell wall diameter of fungal SEVs and hyphae. Ten measurements were taken and averages were calculated for three SEVs and three hyphae per sample. Measurements were performed across three independent biological replicates.

Light Microscopy

Root samples were placed in fixative overnight (4% paraformaldehyde, 2.5% glutaraldehyde in 0.05M phosphate buffer, pH 7.2), before dehydration in a graded ethanol series. Roots were infiltrated and embedded in glycol methacrylate resin using the Agar GMA HEMA kit (Agar Scientific, UK). Embedded samples were sectioned to 4 µm thickness. To visualise plant lignins, sections were stained with 1% w/v potassium permanganate for 10 minutes. To

visualise fungal structures, sections were stained with 1% w/v aniline blue in lactophenol for 30 seconds. Semi-thin LR White resin sections containing *G. hyphopodioides* SEVs (see above) were stained with 1% w/v toluidine blue for 1 minute. All stained sections were mounted onto slides with DPX mounting fluid (Sigma Aldrich®). Sections were imaged using a ZEISS Axio Imager light microscope (ZEISS, Germany).

Fluorescent staining and confocal microscopy analyses

To assess colonisation in whole root pieces, samples were cleared in 10% w/v potassium hydroxide for 5 minutes at 70 °C, before staining with Propidium Iodide (PI) (10 µg/ml) and Wheat Germ Agglutinin, Alexa Fluor™ 488 Conjugate (WGA) (10 µg/ml). To visualise vascular infection by *G. tritici*, transversal root sections were cut by hand using a fine edged razor blade under a dissecting microscope. Confocal microscopy was performed using a ZEISS 780 Confocal Laser Scanning Microscope (ZEISS, Germany). WGA fluorescence was excited at 495 nm and detected at 519 nm. PI fluorescence was excited at 535 nm and detected at 617 nm.

RNA extraction

Following confocal assessment (see above), 1 cm samples at the same stage of fungal colonisation (harvested from the same plate) were pooled together to create a single sample for RNA extraction. RNA was extracted from frozen root material using the E.Z.N.A.® Plant RNA Kit with the associated RNase-free DNase I Set (Omega-Biotek, USA), following the standard protocol provided. RNA quality was assessed based on the RNA Integrity Number (RIN), measured using the Bioanalyser 2100 with the corresponding RNA 6000 Nano Kit (Agilent, USA), as per manufacturer instructions.

Library preparation and sequencing

mRNA library preparation was carried out by Novogene (China) using the Novogene RNA Library Prep Set (PT042) for polyA enrichment. Libraries were sequenced by Illumina NovaSeq to generate 150 bp paired-end reads, with a target of 40 million paired-end reads per sample.

Transcriptome annotation and analysis

Quality control of reads was performed using MultiQC (https://multiqc.info/). Sequence trimming of recognised adaptors was performed using Trimmomatic where appropriate (Bolger et al., 2014). Reads were mapped to the Chinese Spring (IWGSC RefSeq v2.1) (Zhu et al., 2021) using HiSat2 (Kim et al., 2019). To ensure that fungal biomass was consistent among replicates of the same treatment, reads were also mapped to the *G. tritici* genome (Okagaki et al., 2015). Reads were not aligned to *G. hyphopodioides* due to the lack of a high-quality genome. Count determination was performed using FeatureCounts (Liao et al., 2014) on the R Bioconductor platform (https://bioconductor.org/). Three replicates were identified as outliers based on standardised residuals of the percentage of reads mapped to *G. tritici.* Outliers were subsequently excluded from further analyses (table S5).

Library normalisation and differential expression (DE) calling was carried out using the Bioconductor package DESeq2 (Love et al., 2014) in R studio. Gene expression levels were compared between *G. tritici* infected or *G. hyphopodioides* colonised samples and the uninoculated control samples for each time point individually. DE genes were identified by

applying a log2 fold change filter of ≥ 1 or ≤ -1. The DESeq2 implementation of Benjamini-Hochberg (Benjamini & Hochberg, 1995) was used to control for multiple testing ($q<0.05$). Gene Ontology (GO) enrichment analysis was performed for significantly up- and down-regulated wheat genes separately via http://www.geneontology.org, using the Panther classification system.

Validation of gene expression by RT-qPCR

The transcript abundance of selected DEGs was assessed in 5 dpi samples by RT-qPCR. cDNA was synthesised using the SuperScript™ IV Reverse Transcriptase Kit with Oligo (dT) primers (ThermoFisher Scientific, USA), according to the manufacturer's instructions. RT-qPCR was carried out using the PowerTrack™ SYBR Green Master Mix (ThermoFisher Scientific, USA) on the QuantStudio™ 6 Pro Real-Time PCR System (Applied Biosystems™, USA). Relative gene expression levels were calculated using the $2^{-\Delta\Delta CT}$ (Livak) method (Livak & Schmittgen, 2001), following normalisation to the cell division control 48 (CDC48) housekeeping gene (Lee et al., 2014). Primer sequences used in qPCR assays can be found in table S1.

Statistical analyses

Statistical analyses were done using Genstat 20th Edition (VSN International Ltd, Hemel Hempstead, UK). Percentage disease data were analysed using a Generalised Linear Regression Model (GLM) with a binomial distribution and LOGIT link function. Analyses were adjusted for over-dispersion and treatment effects tested using deviance ratios (F-statistics) when the residual mean deviance was greater than 1. Data were back-transformed from the LOGIT scale (using the equation $\exp(x)/(1+\exp(x))$) for graphical presentation. For continuous outcome variables such as plant biomass, data were analysed by Analysis of Variance (ANOVA).

Post-hoc multiple comparisons tests were carried out when more than one interaction was of interest. For multiple comparisons to a single control treatment, Dunnett's post-hoc test was carried out (Dunnett, 1955). For multiple comparisons to more than one control treatment or between multiple treatments, Tukey's multiple comparisons test was carried out.

Results

Hyphal interactions between *G. hyphopodioides* and *G. tritici*

To investigate the role of direct hyphal interaction in the control of take-all disease by *G. hyphopodioides*, a series of fungal confrontation assays were conducted on potato dextrose agar (PDA) plates. Prior to hyphal contact, the individual growth rates of *G. tritici* and *G. hyphopodioides* colonies did not significantly differ from the dual colony controls (table S2). The same was true when the two species were grown in a "sandwich" plate set-up (figure 1A, table S3), suggesting that prior to hyphal contact, neither species produce diffusible antifungal compounds or volatile organic compounds *in vitro*.

When hyphae of the two fungal species interacted, colony growth was restricted and hyphal melanisation was observed in the interaction zone (figure 1A). The observed melanisation occurred 1-2 days following hyphal interaction, suggesting that direct interaction causes hyphal stress in at least one of the interacting species. Colony growth was also restricted when isolates of the same species were confronted, though hyphal melanisation was not observed (figure S2, table S4). Unfortunately, *in planta* interaction studies were not feasible due to difficulties transforming these fungal species (Palma-Guerrero et al., 2021). Nevertheless,

given the *in vitro* data described here, direct fungal interaction alone is unlikely to be the only cause of take-all disease reduction *in planta.*

Pre-treatment with *G. hyphopodioides* provides local control against take-all disease

To investigate the hypothesis that non-pathogenic *G. hyphopodioides* provides protection against take-all disease by induced plant resistance, seedling co-inoculation experiments were carried out under controlled environment conditions. *G. hyphopodioides* inoculum was added to wheat seedlings (cv. Hereward) growing in pots 1 week prior, 2 weeks prior, at the same time as, or 1 week after inoculation with pathogenic *G. tritici.* Characteristic black necrotic root lesions were observed in the *G. tritici* infected plants, whilst previously described "sub-epidermal vesicles" (Osborne et al., 2018) were detected in *G. hyphopodioides* colonised plants (figure 1B).

The data revealed a significant reduction in both take-all disease levels (GLM: $F=25.99$, d.f. 4, 49, $p <0.001$); and *G. tritici* fungal biomass ($F=61.10$, d.f. 4, 38, $p <0.001$) in plants pre-treated with *G. hyphopodioides* 2-weeks prior or 1-week prior to *G. tritici* inoculation (figure 1C, D). Hence, even very early colonisation by *G. hyphopodioides* is sufficient for take-all control. These findings were consistent with additional experiments involving a different *G. tritici* isolate and wheat cultivar (cv. Chinese Spring) (figure S3). In addition, a split-root approach revealed that *G. hyphopodioides*-induced resistance operates at the local, rather than systemic level (figure 1G), with significant disease reduction achieved only in the *G. hyphopodioides* pre-colonised roots ($F=29.44$, d.f. 2, 36, $p=0.007$). Taken together, we demonstrate that local induced plant resistance plays a crucial role in the control of take-all disease by *G. hyphopodioides,* and this response is consistent across both winter and spring wheat types.

In line with this finding, seedlings co-inoculated with *G. hyphopodioides* and *G. tritici* (at the same time) had no effect on take-all disease levels or *G. tritici* fungal biomass. Importantly, adding *G. hyphopodioides* after *G. tritici* resulted in increased levels of take-all disease and *G. tritici* fungal biomass (figure 1C, D). Furthermore, the shoot and root dry biomass of plants in this latter treatment were significantly reduced ($F=6.49$, d.f. 5, 36, $p <0.001$; $F=4.50$, d.f. 5, 36, $p <0.01$, respectively), indicating that seedling health is negatively affected when *G. hyphopodioides* is added to *G. tritici* infected plants (figure 1E, F). These findings should be taken into careful consideration when evaluating the potential of *G. hyphopodioides* as a biocontrol agent.

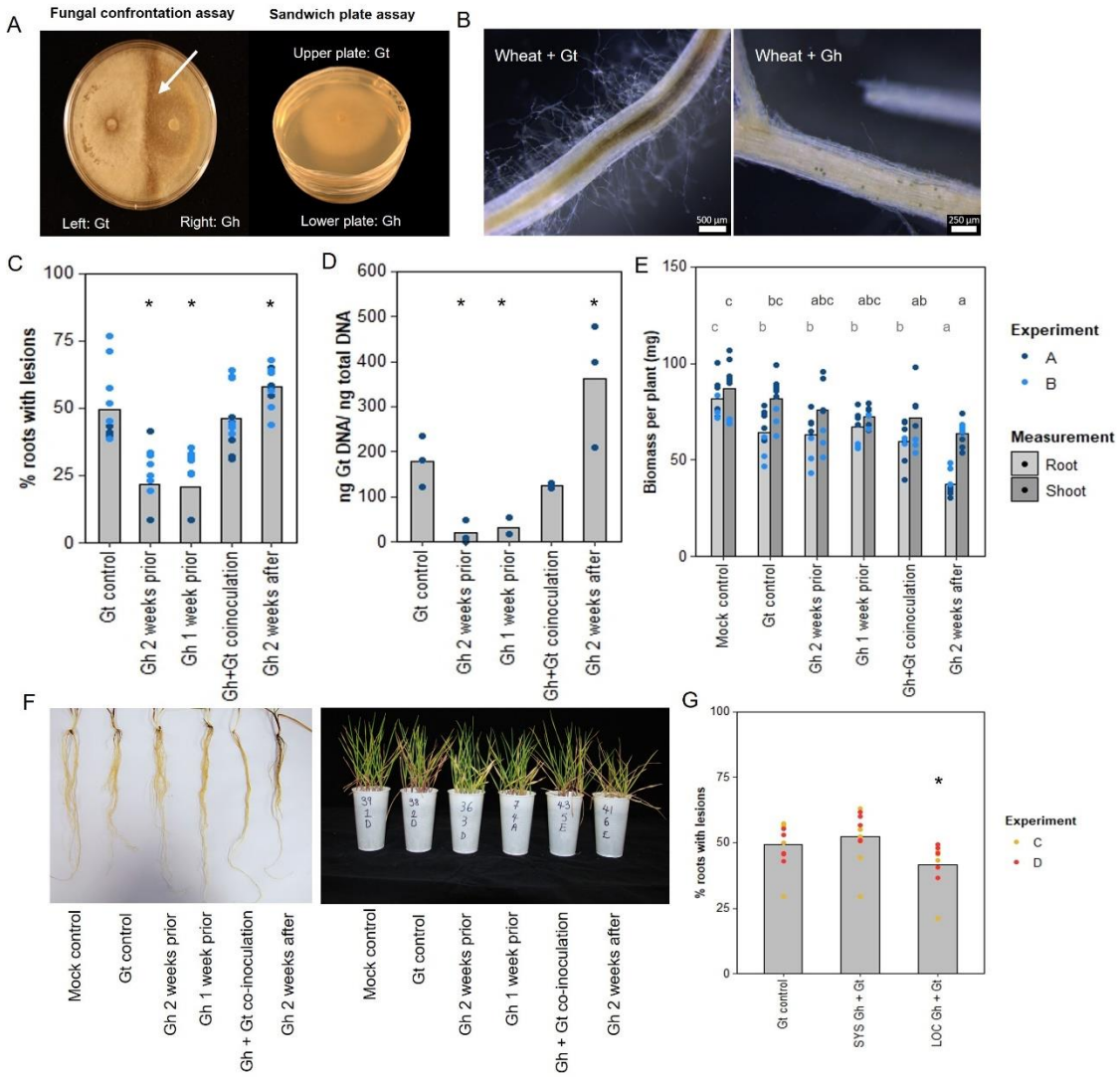

Figure 1. *In vitro* and *in planta* interaction studies involving endophytic *G. hyphopodioides* and pathogenic *G. tritici*. A. *In vitro* fungal interaction assays on PDA plates. Fungal confrontation assays imaged 11 days after establishment, colonies in sandwich plate assays imaged 6 days after establishment. Arrow indicates the zone of melanised hyphae; B. Stereomicroscope images of characteristic *G. tritici* and *G. hyphopodioides* infection symptoms in wheat roots. Arrowheads indicate sub-epidermal vesicles (SEVs); C. Percentage of wheat roots (cv. Hereward) with take-all root lesions in the different co-inoculation treatments; D. *G. tritici* fungal biomass (ng *G. tritici* DNA/ ng total DNA), quantified by qPCR; E. Root and shoot dry biomass (mg); G. The percentage of wheat roots (cv. Chinese Spring) with take-all lesions in split root experiments. All fitted means for percentage responses were back-transformed from the LOGIT scale. Asterisks indicate a significant difference to the *G. tritici* control as calculated by Dunnett's post-hoc test ($p < 0.05$). Letters indicate significant differences as calculated by Tukey's multiple comparisons test ($p<0.05$). Gt= *G. tritici,* Gh= *G. hyphopodioides*, SYS=systemic, LOC=local.

G. hyphopodioides and *G. tritici* produce distinct infection structures in wheat roots

To capture key stages of early fungal colonisation prior to necrotic lesion formation, seedlings were grown in an agar plate system and harvested daily from 2-6 dpi. Three time-points (2, 4 and 5 dpi) were selected for RNA-seq analysis based on the presence of hyphae in different root tissue layers. At 2 dpi, very few hyaline runner hyphae were detected on the root surface

of plants inoculated with either *G. tritici* or *G. hyphopodioides*, and hyphae had not yet penetrated the epidermal cells in either interaction (figure 2A, B). By 4 dpi, hyaline runner hyphae covered a greater area of the root surface (figure S4) and hyphae were detected in epidermal and cortical cells of both *G. tritici* and *G. hyphopodioides* inoculated roots (figure 2A, B). At 5 dpi, hyaline runner hyphae were detected across a large area of the root surface (figure S4) in both fungal treatments. *G. tritici* hyphae infected the stele, whereas *G. hyphopodioides* hyphal growth was arrested in the cortex (figure 2B). Melanised *G. hyphopodioides* macrohyphae were detected in cortical cells, from which previously described but poorly characterised “sub-epidermal vesicles” (SEVs) were formed (figure 2A). Newly formed SEVs could be visualised by WGA staining, whereas mature SEVs, which were no longer connected to an intraradical hypha, could not be visualised by WGA staining (figure S4).

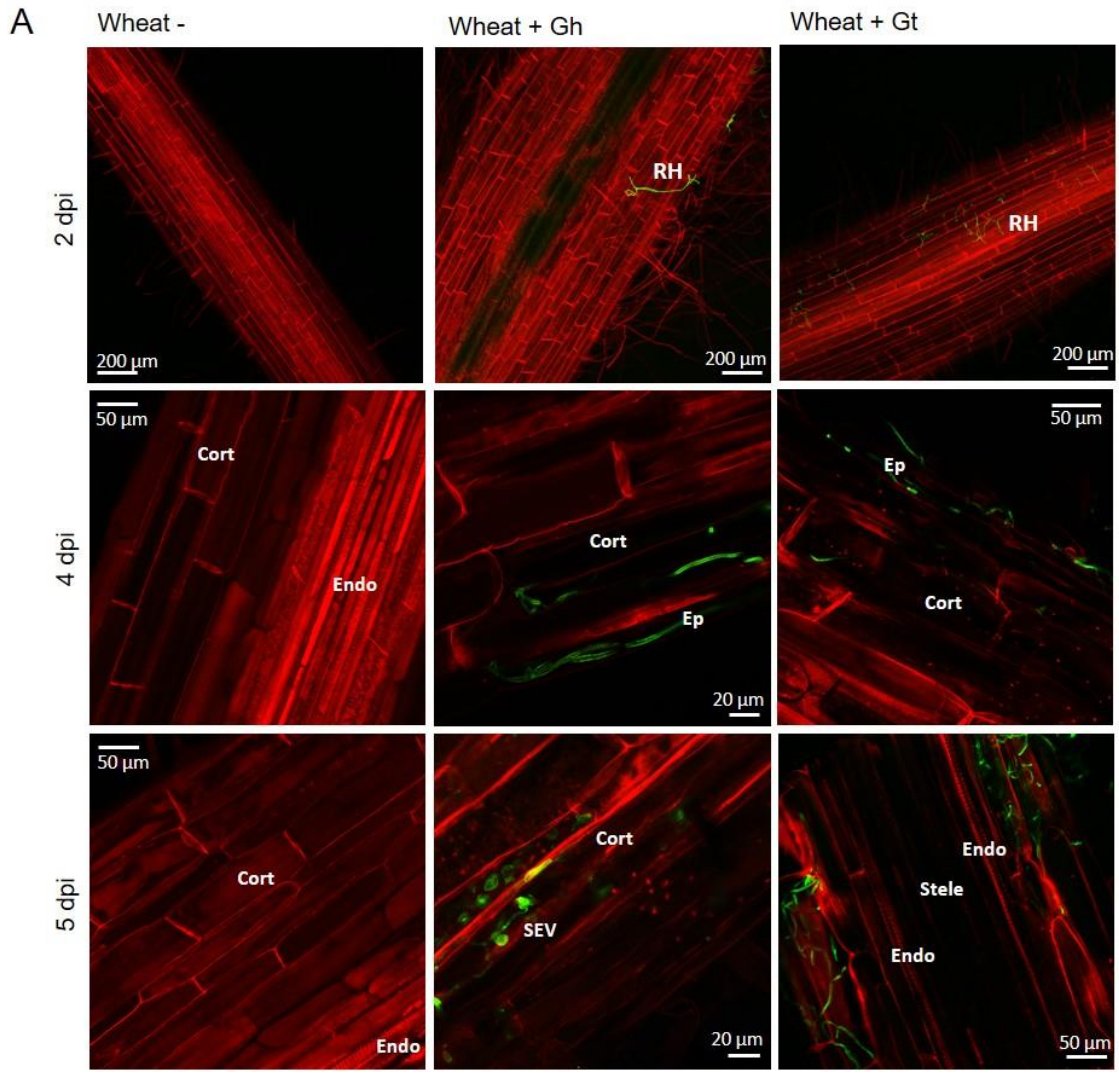

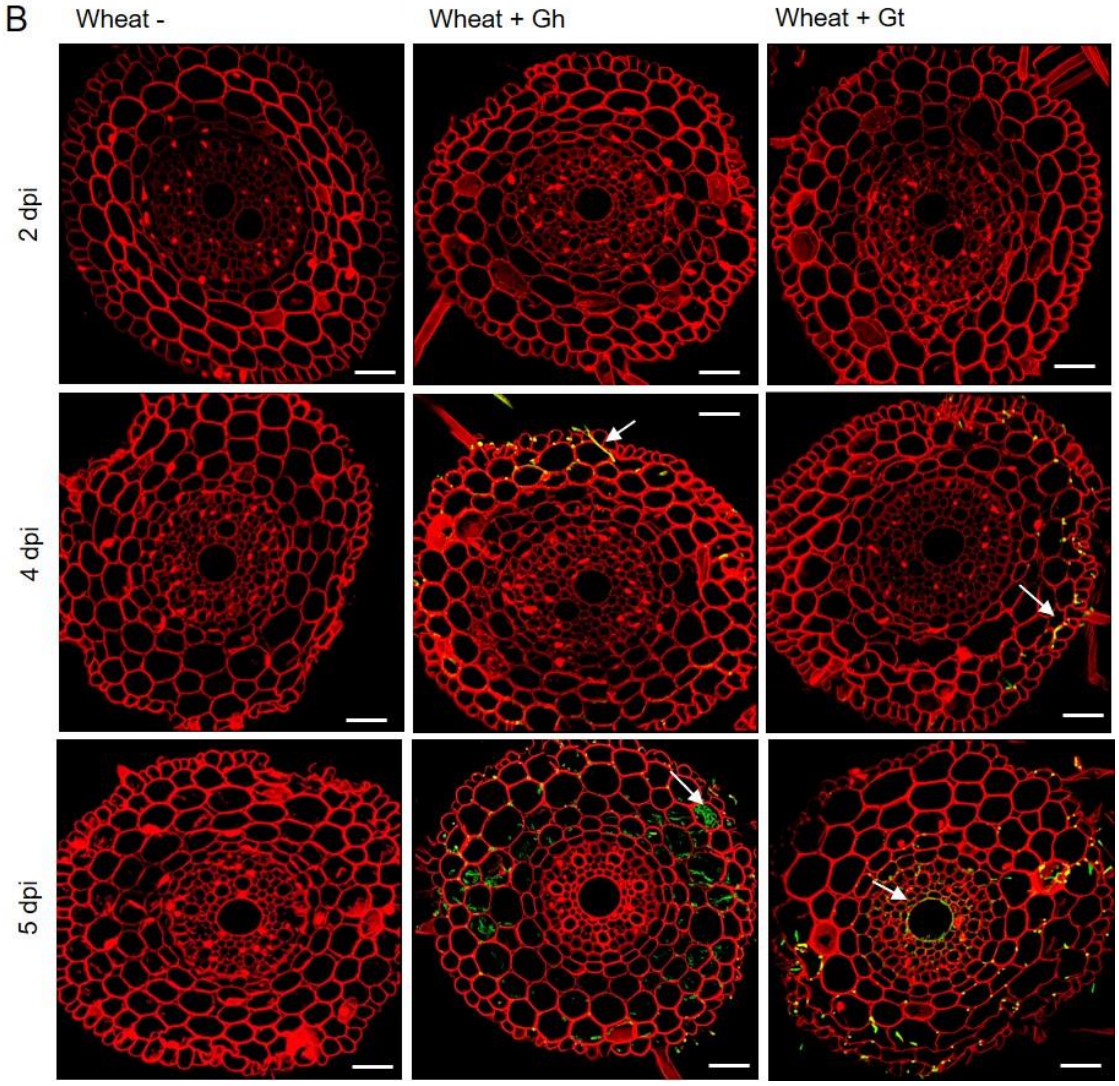

Figure 2. Fluorescence images obtained by confocal microscopy of mock inoculated, *G. hyphopodioides* colonised or *G. tritici* infected wheat roots. (A) Confocal micrographs of whole root pieces demonstrating fungal infection structures. (B) Z- stack images of transversal sections highlighting colonisation of different root cell layers at the key time points selected for RNA sequencing. Gt= *G. tritici,* Gh= *G. hyphopodioides,* RH= runner hyphae, Ep=epidermal cell, Cort= cortical cell, SEV= sub-epidermal vesicle, Endo= endodermal barrier. Arrows in panel B indicate fungal hyphae. Scale bars in panel B represent 50 µm.

To investigate the structure of mature *G. hyphopodioides* SEVs, colonised root tissues were harvested from a 5-week seedling infection pot assay and imaged by transmission electron microscopy (TEM). Comparative analysis of intraradical fungal hypha and SEVs revealed that SEVs contain a large number of putative lipid bodies and a significantly thickened cell wall ($F= 8.3$, d.f. 2, 12, $p<0.01$), comprising two to three layers of differing densities (figure 3A). Surprisingly, SEVs were often found appressed to the plant cell wall and occasionally produced pegs which penetrated the plant cell wall. SEVs with penetration pegs were also produced in seedling infection pot assays with other non-pathogenic *Phialophora* fungi isolated at the Rothamsted Farm (figure 3E, F, G).

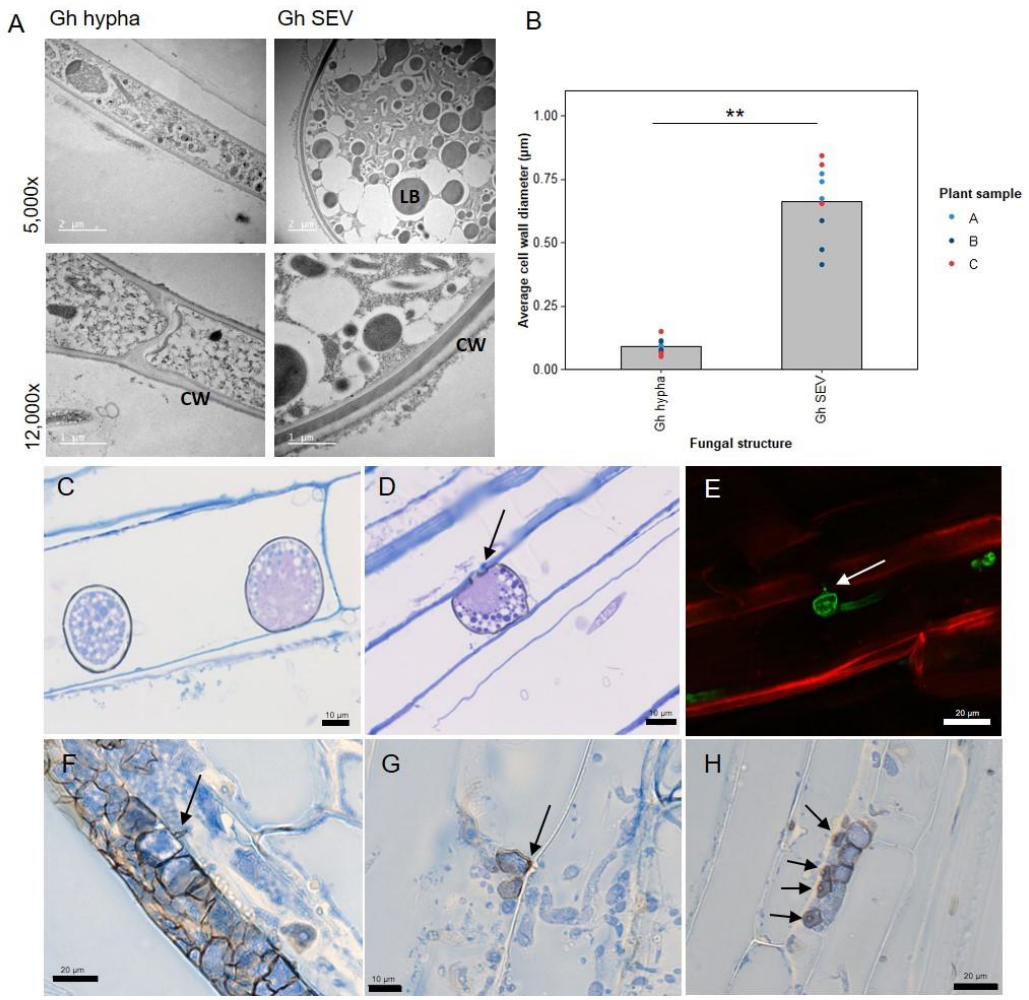

Figure 3. Sub-epidermal vesicles (SEVs) produced by *G. hyphopodioides* (*Gh*) and two other endophytic fungi in wheat roots. A. Transmission electron micrographs (TEM) of *Gh* hyphae (left) and SEVs (right); B. Average cell wall diameter (µm) of *Gh* fungal structures. ***= p<0.001; C, D. Light micrographs of *Gh* SEVs in semi-thin sections, stained with toluidine blue; E. Confocal micrograph of *Gh* SEV; F. Light micrograph of SEVs produced by an unnamed *Magnaporthaceae* sp. Sample embedded in resin, 4 µm section thickness, stained with aniline blue; G, H. SEVs produced by close relative *Slopeiomyces cylindrosporus.* Samples embedded in resin, 4 µm section thickness, stained with aniline blue. Arrows=SEV penetration pegs; CW=plant cell wall; LB=putative lipid body.

G. hyphopodioides colonisation and *G. tritici* infection induces a core subset of wheat response genes

Three time-points (2, 4 and 5 dpi) spanning key stages of early fungal colonisation were selected for RNAseq analysis based on detailed confocal microscopy of harvested root samples. Principal Component Analysis (PCA) of sample distances demonstrated a good level of clustering between biological replicates, though *G. tritici* infected samples exhibited comparatively higher levels of variation (figure 4A). Gene expression levels were compared between *G. tritici* infected / *G. hyphopodioides* colonised plants and the uninoculated control plants at each time point individually. As expected, the number of differentially expressed genes (DEGs) between the uninoculated control and *G. tritici* infected / *G. hyphopodioides* colonised plants was low at 2 dpi (77 and 62, respectively) (figure 4B). By 4 dpi, *G. tritici* infection and *G. hyphopodioides* colonisation resulted in the differential expression of 1061

and 1635 genes, respectively, with 839 genes differentially expressed (DE) in response to both fungi. At 5 dpi, a striking number of genes were DE in response to *G. hyphopodioides* colonisation (7532), whereas the number of DEGs in response to *G. tritici* infection (1074) showed little change compared to 4 dpi. Surprisingly, a mere 3% of DEGs were unique to *G. tritici* infection at 5 dpi (figure 4C). This finding indicates that there is a core set of genes which are DE in response to both *G. hyphopodioides* and *G. tritici*. However, this core set of genes makes up only a small proportion (14%) of all genes DE in response to *G. hyphopodioides* at 5 dpi.

By performing gene ontology (GO) enrichment analysis on this core set of genes, we identified highly enriched biological process terms including isoprenoid biosynthesis, plant response to biotic stimulus and phenylpropanoid metabolic process (figure 4D). Of particular interest was the plant response to biotic stimulus term, which comprised 42 DE genes, 14 of which encoded proteins containing small cysteine-rich protein (SCP)-domains, often associated with pathogenesis-related proteins. Six genes encoded chitinases, two encoded wound induced proteins (WIN) and a further four encoded protein kinase domain-containing proteins, thus indicating a clear defence response to both fungi (table S6). Highly enriched molecular function terms included chitinase activity, manganese ion binding and oxidoreductase activity (figure 4E). Genes relating to UDP-glucose transmembrane transport were highly enriched in both biological process and molecular function terms, suggesting that UDP-glucose signalling plays an important role in the wheat response to pathogenic and non-pathogenic *Magnaporthaceae* species, perhaps by acting as a DAMP (Henry Christopher & Van den Ende, 2018).

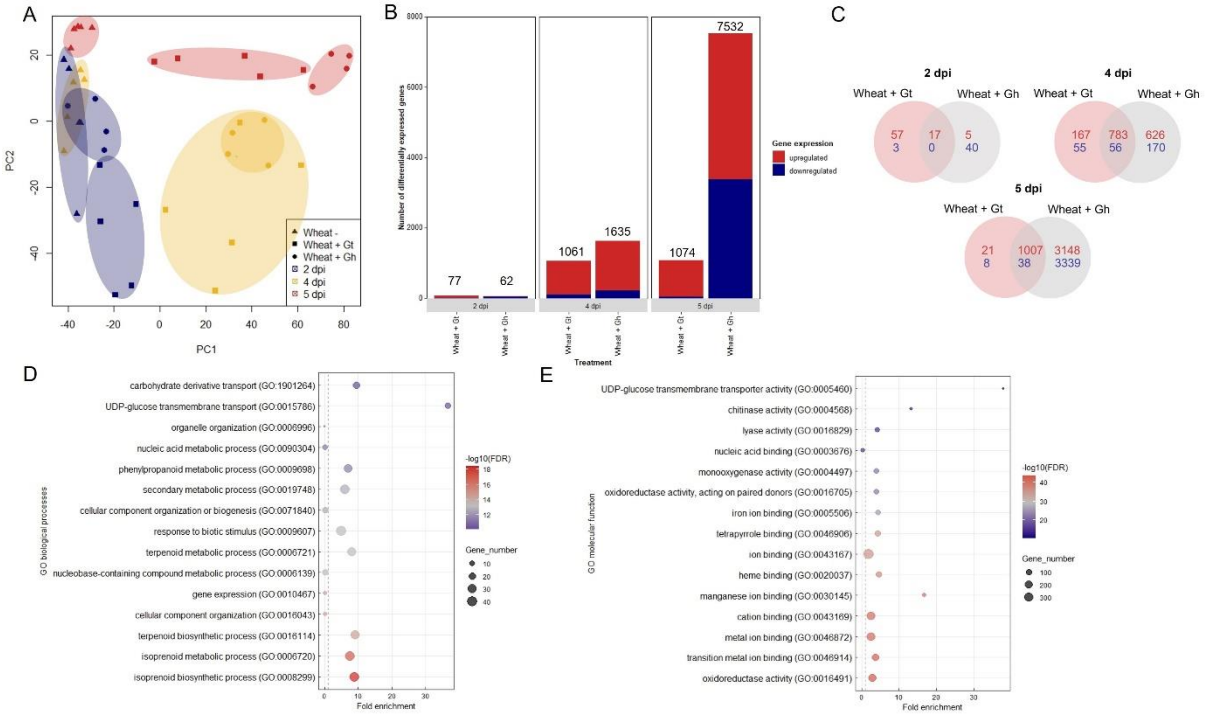

Figure 4. Transcriptional profiling of *G. hyphopodioides* colonised and *G. tritici* infected wheat roots. A. Principal Component Analysis (PCA) plot of sample distances based on vsd transformed gene count data. Generated using DeSeq2 in R studio. Data points have been categorised by shape and colour to denote treatment and time point, respectively; B. The number of differentially expressed genes (DEGs) in wheat colonised by either *G. hyphopodioides* or *G. tritici* across three key time points; C. Venn diagram highlighting unique and shared DEGs across treatments; Top 15 GO enriched biological process (D) and GO molecular function (E) terms among core DEGs in *G. hyphopodioides* and *G. tritici* infected plants at 5 dpi.

Wheat transcriptional remodelling during fungal infection

To investigate the changes in the wheat transcriptome during the progression of *G. hyphopodioides* and *G. tritici* infection, biological process GO terms were compared between each time point and the top ten newly enriched terms were identified. Due to the lack of downregulated genes in *G. tritici* colonised plants at 2 dpi, enriched terms could not be identified. However, upregulated terms related to lipid and diterpenoid biosynthesis and metabolism, suggesting a key role in the early plant response to *G. tritici* infection (figure 5A). At 2 dpi, key downregulated terms in *G. hyphopodioides* colonised plants included nicotianamine biosynthetic process and amine biosynthetic process (figure 5B). At 4 dpi, new highly enriched terms for upregulated genes in *G. tritici* infected plants included response to stimulus, carbohydrate derivative transport and chitin metabolic/catabolic process. Terms from downregulated genes included response to oxygen-containing compounds, response to nitrate and nitrate transport, potentially indicating a role of reactive oxygen/nitrogen species in the plant defence response against *G. tritici* (Zaninotto et al., 2006). New highly enriched terms for upregulated genes in *G. hyphopodioides* colonised plants included cinnamic acid metabolic/biosynthetic process, L-phenylalanine metabolic process, phenylpropanoid metabolic process and aromatic amino acid family metabolic process, suggesting that lignin biosynthesis is important at this time point. Downregulated terms included hydrogen peroxide metabolic/catabolic process, cell wall biogenesis and response to toxic substance (figure 5B).

At 5 dpi, new upregulated terms in *G. tritici* infected plants included cinnamic acid metabolic/biosynthetic process, L-phenylalanine metabolic process and olefinic compound biosynthetic process, suggesting that lignin biosynthesis is also involved in the defence response to *G. tritici*, though at a later stage than *G. hyphopodioides. G. hyphopodioides* downregulated terms included gene expression, plant-type cell wall organisation or biogenesis, RNA metabolic process and sexual reproduction. Upregulated terms included response to wounding, regulation of defence responses and regulation of the jasmonic acid signalling pathway (figure 5B).

The jasmonic acid signalling GO term comprised 26 DEGs (out of a total of 77 known genes in wheat), all of which were TIFY transcription factors, involved in the cross-talk between JA and other phytohormones (Singh & Mukhopadhyay, 2021). In contrast, just three TIFY transcription factors were DE in *G. tritici* infected plants compared to the control. Although not identified by GO enrichment analysis, we also investigated the expression of JA biosynthesis genes. In total, 23 JA biosynthesis-related genes were DE (17 up/ 6 down) in response to *G. hyphopodioides* at 5 dpi. The list included lipoxygenase (LOX), allene oxide synthase (AOS) and AOS-like, 12-oxophytodienoate reductase (OPR) and OPR-like, and 3-ketoacyl-CoA thiolase (KAT-like) genes. Of these genes, only one was differentially expressed in response to *G. tritici* (LOX8_TraesCS7B02G145200) (figure S6). Because JA and ET signalling are often closely linked, we also investigated genes involved in ET biosynthesis and signalling. Five ACC-oxidase (ACO-like) genes were upregulated in response to *G. hyphopodioides* by 5 dpi. In addition, 22 ethylene responsive transcription factor-like (ERF-like) genes, key integrators of downstream ET and JA signal transduction pathways (Lorenzo et al., 2003), were DE (19 up/ 3 down) in response to *G. hyphopodioides* by 5 dpi. In contrast, four ERF-like genes were upregulated at 4 dpi and two were upregulated at 5 dpi in *G. tritici* infected roots compared to the control (figure S6). Thus, unlike in EMR by non-pathogenic *Fusarium* species, *G. hyphopodioides*-induced resistance is potentially mediated, at least to some extent, by the JA/ET signalling pathway.

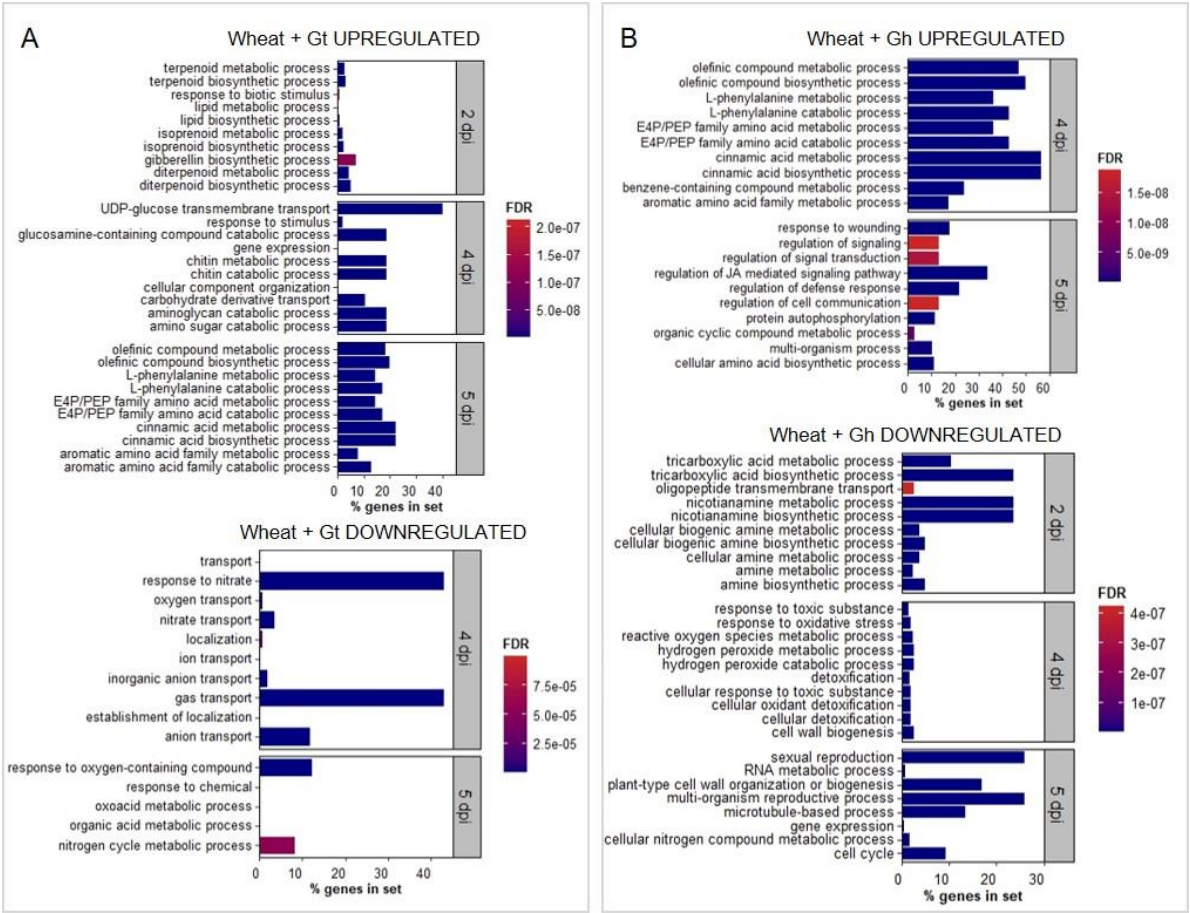

Figure 5. The top ten newly enriched biological process gene ontology (GO) terms at each time point. A. Upregulated and downregulated terms in *G. tritici* infected root samples. B. Upregulated and downregulated terms in *G. hyphopodioides* colonised root samples. Percentage of genes in a set represents the percentage of DE genes out of the total number of known genes in that category, according to the Panther classification system.

G. hyphopodioides colonisation results in the early induction of lignin biosynthesis genes

Previous studies have reported higher levels of cell wall lignification in response to colonisation by several non-pathogenic *Magnaporthaceae* species compared to infection by *G. tritici* (Huang et al., 2001; Speakman & Lewis, 1978). To investigate root lignification in response to *G. hyphopodioides* and *G. tritici*, we explored the expression of key genes involved in the lignin biosynthesis pathway in wheat (figure 6A). In accordance with the findings of the GO analysis, *G. hyphopodioides* colonisation resulted in the earlier upregulation of lignin biosynthesis genes compared to *G. tritici*, with key genes such as arogenate dehydratase (ADT), phenylalanine ammonia-lyase (PAL), cinnamate 4-hydroxylase (4CL) and cinnamoyl-CoAreductase (CCR) significantly upregulated at 4 dpi (figure 6B). However, two of eight caffeic acid *O*-methyltransferase (COMT) genes detected were already significantly upregulated in response to *G. tritici* at 2 dpi. Interestingly, the remaining COMT genes were strongly downregulated in response to *G. hyphopodioides* by 5 dpi, suggesting a decrease in the proportion of syringyl (S)-lignin. Changes in S lignin composition can drastically alter the outcome of plant-pathogen interactions, though conflicting results have been reported (Höch et al., 2021; Ma et al., 2018; Quentin et al., 2009). Most striking however, was the significant upregulation of 37 PAL genes in response to *G. hyphopodioides*, compared to the upregulation of just 12 PAL genes in response to *G. tritici* at 5 dpi.

To visualise lignification of infected root tissues, potassium permanganate staining was performed on transversal sections. The overall level of root lignification varied within *G. hyphopodioides* colonised and *G. tritici* infected samples, with some sections difficult to distinguish from the uninoculated control. However, heavily colonised cells exhibited cell wall thickenings and increased lignin levels when compared to uncolonised neighbouring cells, indicating a strong local response. Plant lignitubers, lignified callose deposits surrounding hyphal tips (Huang et al., 2001), were often detected in cells containing fungal hyphae, though these structures were more common in *G. tritici* infected samples. Surprisingly, *G. hyphopodioides* colonisation did not result in visible lignification of the stele or endodermal barrier compared to the control, and lignification levels did not appear to be greater than in *G. tritici* infected tissues (figure 6C). This finding contrasts with previously published microscopy studies into the infection mechanisms of non-pathogenic *Magnaporthaceae* species, though *G. hyphopodioides* was not among the species previously tested (Huang et al., 2001; Speakman & Lewis, 1978).

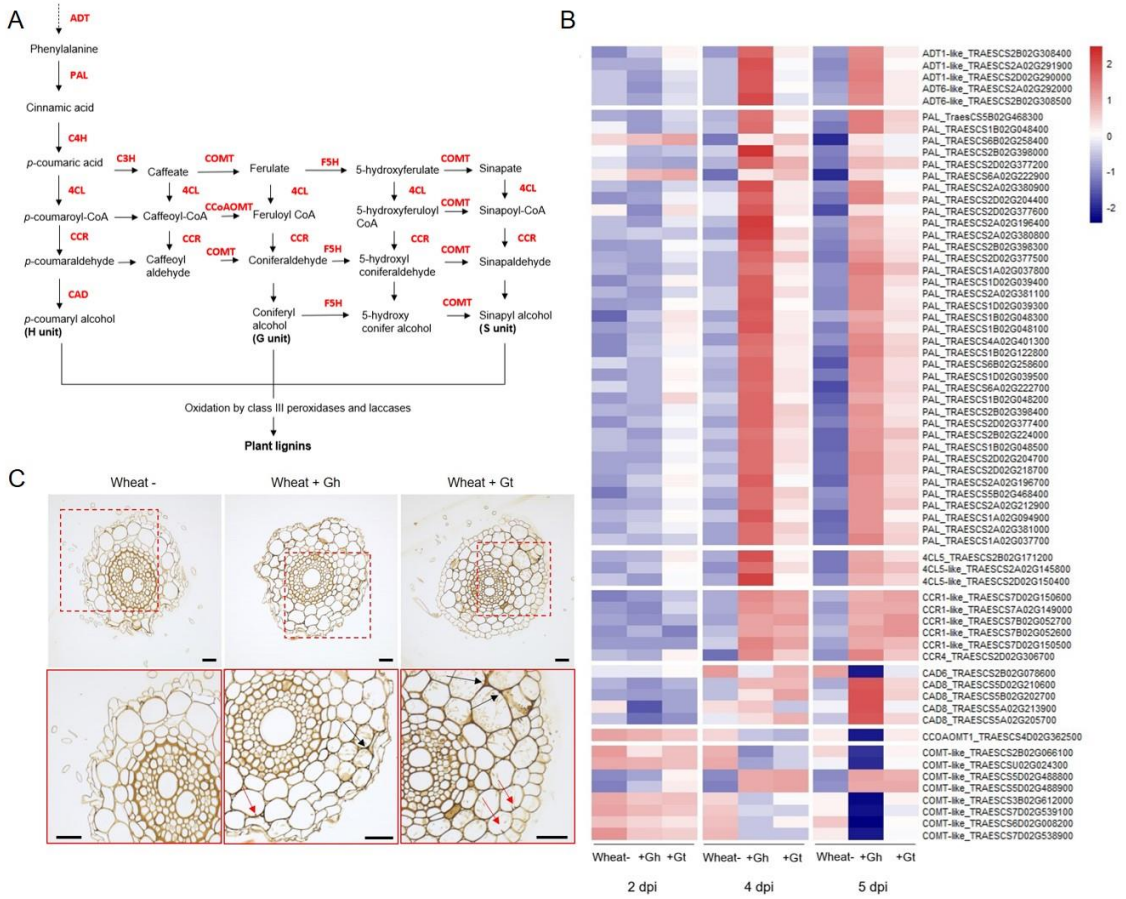

Figure 6. Lignin biosynthesis in response to *G. hyphopodioides* and *G. tritici* infection. A. Schematic of the lignin biosynthesis pathway in plants (adapted from Nguyen et al., 2016); B. Expression of key genes involved in the lignin biosynthesis pathway, based on LOG transformed normalised gene counts; C. Micrographs of transversal root sections stained with potassium permanganate for the visualisation of cell wall lignification in response to fungal infection at 5 dpi. Black arrows indicate lignified cell wall thickenings, red arrows indicate plant lignitubers. Scale bars represent 50 µm. arogenate dehydratase (ADT); phenylalanine ammonia-lyase (PAL); cinnamate 4-hydroxylase (C4H); 4-coumarate CoA ligase (4CL); quinateshikimate *p*-hydroxycinnamoyltransferase (HCT); *p*-coumaroylshikimate 3′-hydroxylase (C3′H); caffeoyl-CoA *O*-methyltransferase (CCoAOMT); cinnamoyl-CoAreductase (CCR); ferulate 5-hydroxylase (F5H); cinnamyl alcohol dehydrogenase (CAD); caffeic acid *O*-methyltransferase (COMT).

Cell-wall related defence mechanisms are likely to play an important role in the control of take-all disease by *G. hyphopodioides*

As identified by GO enrichment analysis, *G. hyphopodioides* colonisation resulted in the significant downregulation of 124 genes involved in cell wall organisation and biogenesis by 5 dpi (out of 1122 total known genes involved in cell wall organisation and biogenesis in wheat). In contrast, *G. tritici* infection did not lead to the differential expression of any genes within the cell wall organisation and biogenesis GO term. Focussing on the top 30 DE genes within this GO term in *G. hyphopodioides* colonised plants at 5 dpi, we identified six xyloglucan endotransglycosylases/hydrolases (XTH) genes, three cellulose synthase-like A-like (CSLA) genes, one cellulose synthase-like F (CSLF) gene and three fasciclin-like arabinogalactan (FLA) genes (figure 7A). Though just one cellulose synthase-like (CESA) gene was present in the list of top 30 DEGs, a total of 10 CESA genes were downregulated at 5 dpi (table S7). To validate gene expression, we identified key cell-wall related genes where all three wheat homoeologues were highly downregulated in the RNA-seq dataset (figure 7B). qPCR analyses revealed that, as expected, cell-wall related genes CESA7-like, COBL-5D, FLA11 were downregulated in *G. hyphopodioides* colonised plants (figure 7C).

A

Gene ID	Gene name	Log2FC	padj
TraesCS5A02G548500	XTH	-5.66	4.27E-22
TraesCS7A02G363000	XTH	-4.52	1.51E-17
TraesCS7D02G360100	XTH	-5.10	2.71E-10
TraesCS7D02G294300	CSLF6	-3.49	4.39E-10
TraesCS4B02G383000	XTH	-3.39	4.97E-10
TraesCS4D02G358700	XTH	-3.81	5.00E-10
TraesCS7B02G265000	XTH	-6.31	5.28E-10
TraesCS6A02G169200	CSLA1-like	-4.05	6.71E-09
TraesCS6B02G197200	CSLA1-like	-3.61	7.97E-09
TraesCS3B02G376800	EXPA2	-3.43	1.03E-08
TraesCS3B02G120700	FLA11	-4.06	1.13E-08
TraesCS2A02G082500	IRX9	-4.36	1.35E-08
TraesCS6D02G158600	CSLA1	-3.57	5.19E-08
TraesCS2D02G091400	Unknown	-4.14	7.54E-08
TraesCS5D02G137300	GT3	-3.10	1.77E-07
TraesCS3D02G105500	FLA11	-3.80	2.79E-07
TraesCS2D02G080400	IRX9	-4.33	3.13E-07
TraesCS2A02G153000	PAE	-2.86	3.45E-07
TraesCS5A02G143800	GAUT7	-3.65	4.99E-07
TraesCS1D02G404700	FLA6	-3.28	1.03E-06
TraesCS6A02G131900	IRX15-like	-5.26	1.27E-06
TraesCS2D02G099900	PME	-8.49	1.48E-06
TraesCS4A02G227100	GXM-like	-7.37	1.62E-06
TraesCS5D02G107900	COBL-5B	-3.33	2.20E-06
TraesCS5D02G280400	CTL1	-2.22	2.68E-06
TraesCS6D02G121700	IRX15-like	-4.45	3.22E-06
TraesCS5A02G129800	GT3	-2.80	5.03E-06
TraesCS1D02G111600	FLA11	-7.80	7.85E-06
TraesCS4D02G086700	GXM1-like	-4.24	8.06E-06
TraesCS1B02G167200	CESA7-like	-3.04	9.85E-06

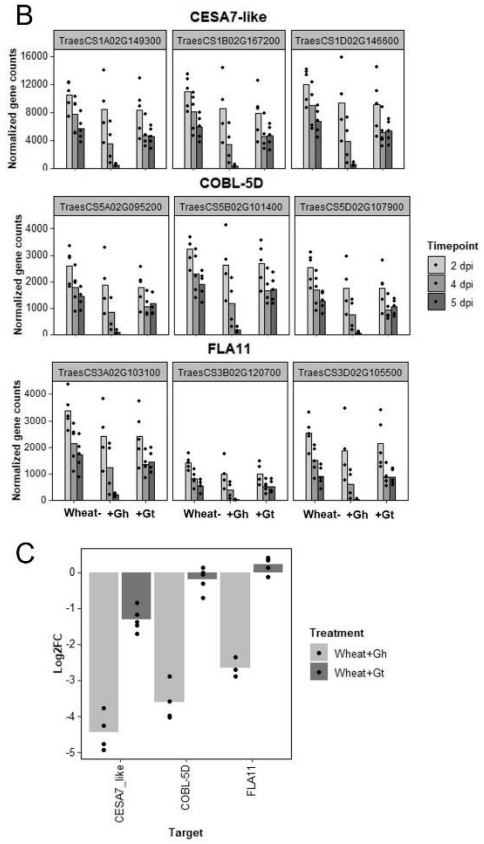

Figure 7. Colonisation by *G. hyphopodioides* results in local downregulation of cell-wall related genes. A. The top 30 most differentially expressed genes relating to cell wall organisation and biogenesis in *G. hyphopodioides* colonised plants at 5 dpi. Ordered by significance (padj); B. Gene counts of selected genes across time points; C. qPCR validation of selected genes in 5 dpi samples.

Discussion

The take-all fungus causes one of the most important root diseases of wheat worldwide because effective control methods are lacking (Palma-Guerrero et al., 2021). The biocontrol potential of several non-pathogenic *Magnaportha*ceae species has been reported as early as the 1970s (Deacon, 1973, 1976; Wong & Southwell, 1980). However, the precise mechanism of control and the molecular pathways underpinning these interactions have remained underexplored. In this study, we show that induced plant resistance mechanisms play a key role in *G. hyphopodioides*-mediated disease reduction. Furthermore, we demonstrate that these resistance mechanisms operate at a local scale, with effective disease protection conferred in roots pre-treated with *G. hyphopodioides*. However, adding *G. hyphopodioides* after *G. tritici* resulted in increased take-all disease levels, thereby posing a significant risk for field application. The potential for *G. hyphopodioides* to become pathogenic in wheat and/or other cereal crops requires careful investigation. Nevertheless, farmers may exploit the disease suppression ability of *G. hyphopodioides* by growing wheat cultivars known to support natural populations, particularly when placed early in wheat rotations (Osborne et al., 2018).

In support of early studies into non-pathogenic *Magnaporthaceae* species (Holden, 1976; Speakman & Lewis, 1978), we observed that while the root infecting pathogen *G. tritici* can grow into the vascular tissues of wheat, growth of endophytic *G. hyphopodioides* is limited to the inner cortex. In addition, we observed characteristic SEVs in *G. hyphopodioides* colonised wheat roots. TEM analysis of *G. hyphopodioides* SEVs revealed that the structures share key similarities with fungal chlamydospores, both being characterised by a thickened, multi-layered cell wall and abundant lipid bodies. Contrastingly, *G. hyphopodioides* SEVs were occasionally found to produce pegs which penetrated the plant cell wall, suggesting a role in infection. The closely related rice leaf blast pathogen *Magnaporthe oryzae,* is also reported to form SEVs in cereal roots. Although primarily a foliar pathogen, *M. oryzae* can infect root tissues (Dufresne & Osbourn, 2001; Marcel et al., 2010), producing brown spherical structures resembling SEVs in epidermal and cortical cells of rice. Interestingly, SEV-like structures (referred to as microsclerotia) are also common among dark septate endophytes (DSE), a diverse group of root colonising ascomycete fungi (Ban et al., 2012; Knapp et al., 2018). For instance, *Harpophora oryzae*, a DSE of rice which shows biocontrol potential against rice blast disease, produces SEV-like structures which seem to be involved in root infection (Su et al., 2013). Further investigation is needed to determine whether fungal SEVs may in fact play a more active role in the infection biology of diverse root infecting fungi.

Though transcriptional studies of the *G. tritici*-wheat pathogen system have been carried out for both host (Kang et al., 2019; Yang et al., 2015; Zhang et al., 2020) and pathogen (Gazengel et al., 2020; Kang., 2019), this is not the case for the *G. hyphopodioides*-wheat interaction. To investigate early wheat responses to *G. tritici* infection and uncover the local plant defence mechanisms responsible for *G. hyphopodiodes*-induced disease control, we performed comparative transcriptome profiling of *G. hyphopodioides* colonised and *G. tritici* infected wheat using a precision inoculation method. Colonisation by non-pathogenic *G. hyphopodioides* triggered extensive transcriptional reprogramming in colonised root tissues, as determined by the identification of over 7500 differentially expressed genes (DEGs) at 5 dpi, almost half of which were downregulated. In contrast, *G. tritici* infection resulted in far fewer DEGs, the majority of which were upregulated. Interestingly, almost all DEGs identified in response to *G. tritici* infection were also shared with the wheat response to *G. hyphopodioides* colonisation. Despite triggering a significant defence response, *G. tritici* successfully causes disease, suggesting an ability to either suppress or overcome the local plant defences triggered. Therefore, future studies should focus on the elucidation of *G. tritici* effectors, which no doubt contribute to *G. tritici* pathogenicity. One such effector, the ortholog of the barley powdery mildew effector gene BEC1019, has already been associated with *G. tritici* virulence in wheat (Zhang et al., 2019).

Strikingly, 11% of all known cell wall organisation/biogenesis related genes in wheat were downregulated in *G. hyphopodioides* colonised plants at 5 dpi. Impairment of cell wall integrity (CWI) by pathogen invasion triggers the release of antimicrobial compounds and Damage-Associated Molecular Patterns (DAMPs), the latter inducing plant innate immune responses upon recognition by plant Pattern Recognition Receptors (PRRs) (Miedes et al., 2014). In this study, *G. hyphopodioides* colonisation triggered the downregulation of 13 fasciclin-like arabinogalactan (FLA) genes and 18 xyloglucan endotransglucosylase/hydrolase (XTH) genes. FLA proteins contain a putative cell adhesion domain which may link the cell membrane and the cell wall. FLA mutants in Arabidopsis exhibit a range of phenotypes including reduced cellulose content, altered secondary cell-wall deposition and reduced tensile strength (Ashagre et al., 2021). XTH genes are also involved in the maintenance of CWI; these genes encode xyloglucan modifying enzymes which cleave xyloglucan chains to enable cell wall expansion or alter cell wall strength (Cosgrove, 2005). In addition, we detected the downregulation of 10 CESA genes. Though the exact mechanism is not yet known, a number of studies in Arabidopsis indicate a link between CESA expression, CWI and disease resistance. Mutations in the CESA4, CESA7 and CESA8 genes, required for secondary cell wall formation in Arabidopsis, confer enhanced resistance to the necrotrophic fungus *Plectrosphaerella cucumerina* and the biotrophic bacterium *Ralstonia solanacearum* (Hernández-Blanco et al., 2007). In addition, *Fusarium oxysporum* root infection of Arabidopsis resulted in the downregulation of various CESAs, resulting in an alteration in primary cell wall cellulose and contributed to disease resistance (Menna et al., 2021). Furthermore, mutations in CESA genes trigger the activation of defence responses and the biosynthesis of lignin, regulated at least in part, by the jasmonic acid (JA) and ethylene (ET) signalling pathways (Caño-Delgado et al., 2003). A link between JA/ET signalling and reduced cellulose levels has also previously been reported by Ellis et al., (2002). Thus, our finding that *G. hyphopodioides* colonisation results in the local deposition of lignin and the upregulation of JA/ET signalling genes is pertinent. Further investigation is required to determine whether the disruption of CWI mechanisms directly triggers the activation of JA/ET mediated defence pathways.

In summary, we demonstrate rapid and extensive transcriptional reprogramming in *G. hyphopodioides* colonised wheat roots, characterised by the strong induction of diverse plant defence mechanisms. We propose that the collective effect of these defence mechanisms, particularly relating to cell-wall mediated resistance, are responsible for *G. hyphopodioides*-mediated take-all control. Due to the lack of high-quality annotated *G. tritici* and *G. hyphopodioides* genomes, comparative analysis of fungal gene expression during *G. hyphopodioides* colonisation and *G. tritici* infection was not possible in this study. When combined with the RNA-seq dataset presented here, future genome sequencing projects will no doubt facilitate the investigation of novel *G. tritici* pathogenicity factors. In addition, further analysis of non-pathogenic and pathogenic fungi within the diverse *Magnaporthaceae* family may help to address wider questions relating to pathogen organ specificity, conserved root infection strategies and the determination of fungal pathogenicity.

Supplementary data

Table S1. qPCR primer sequences

Table S2. Summary statistics and ANOVA analysis of the av erage colony diameter of *G. hyphopodioides* and *G. tritici* when plated as single or dual colonies compared to *G. hyphopodioides* vs. *G. tritici* confrontation assays.

Table S3. Summary statistics and ANOVA analysis of the average colony diameter of *G. tritici* after 6 days of growth in a sandwich plate bioassay.

Table S4. List of fungal isolates used in *G. hyphopodioides* and *G. tritici* intra-species confrontation assays.

Table S5. Mapping statistics for all RNA sequencing samples.

Table S6. Full list of genes involved in the GO term “response to biotic stimulus”.

Table S7. Full list of predicted cellulose synthase (CESA) genes downregulated in response to *G. hyphopodioides* at 5 dpi.

Figure S1. Schematic showing the root infection protocol and root areas sampled.

Figure S2. *G. hyphopodioides* and *G. tritici* intra-species confrontation assays on potato dextrose agar (PDA).

Figure S3. The percentage of wheat roots with take-all lesions and amount of *G. tritici* fungal biomass (pg *G. tritici* DNA/ ng total DNA) with and without *G. hyphopodioides* pre-treatment.

Figure S4. Fluorescence images obtained by confocal microscopy showing runner hyphae on the root surface at key time points selected for RNA sequencing.

Figure S5. Confocal and transmitted light overlays showing *G. hyphopodioides* SEVs and melanised runner hyphae with and without WGA staining.

Figure S6. The expression of JA and ET related genes in response to *G. hyphopodioides* (Gh) colonisation and *G. tritici* (Gt) infection.

Acknowledgements

We thank Smita Kurup and Hannah Walpole (Plant Sciences for the Bioeconomy, Rothamsted Research) for advice and assistance with fluorescent staining and confocal microscopy of wheat roots; Jess Hammond (Protecting Crops and the Environment, Rothamsted Research) for help with fungal isolations and plant care; Matthew Dickinson (University of Nottingham) for his feedback on the project, and Gabriel Ferreras Garrucho (Crop Science Centre, University of Cambridge) for help with figure generation.

Author contributions

TC, JPG and KHK conceived the project and planned the experiments. TC carried out the plant inoculations, RNA extractions, confocal microscopy, light microscopy, cDNA synthesis and statistical analyses. DS carried out MultiQC, read mapping and count determination. WC and TC performed the qPCR validations. SC guided statistical analyses. GC collected the fungal isolates used in this study and assisted with seedling pot infection assays. EV processed samples for TEM and performed ultrathin sectioning. EV and TC imaged ultrathin sections by TEM. KH stained and imaged SEVs in semi-thin sections by light microscopy, and performed the lignin staining of colonised root tissues. JPG and WC carried out the split-root experiments. VM assisted with the design of wheat co-inoculation experiments. TC, DS, JPG and KHK wrote the manuscript.

Conflicts of interest

The authors have no conflicts of interest to declare.

Funding

TC was supported by the Biotechnology and Biological Sciences Research Council (BBSRC) funded University of Nottingham Doctoral Training Programme (BB/M008770/1). JPG, DS and KHK were supported by the BBSRC Institute Strategic Programme (ISP) Grant, Designing Future Wheat (BBS/E/C/000I0250). In addition, DS is supported by the BBSRC ISP Grant

(BB/CCG2280/1) and KHK by the BBSRC ISP Grant, Delivering Sustainable Wheat (BB/X011003/1). GC is supported by the defra funded Wheat Genetic Improvement Network, WGIN (CH0109).

Data availability

Raw RNA-seq reads are publicly available at the NCBI Gene Expression Omnibus (GEO) under accession GSE242417.

References

Ashagre, H., Zaltzman, D., Idan-Molakandov, A., Romano, H., Tzfadia, O., & Harpaz-Saad, S. (2021). FASCICLIN-LIKE 18 Is a New Player Regulating Root Elongation in Arabidopsis thaliana. *Frontiers in Plant Science*, *12*, 391. https://doi.org/10.3389/FPLS.2021.645286/BIBTEX

Asher, M. J. C., & Shipton, P. J. (1981). *Biology and control of take-all* (M. J. C. Asher & P. J. Shipton, Eds.). London Academic Press.

Ban, Y., Tang, M., Chen, H., Xu, Z., Zhang, H., & Yang, Y. (2012). The Response of Dark Septate Endophytes (DSE) to Heavy Metals in Pure Culture. *PLoS ONE*, *7*(10). https://doi.org/10.1371/journal.pone.0047968

Benjamini, Y., & Hochberg, Y. (1995). Controlling the False Discovery Rate: A Practical and Powerful Approach to Multiple Testing. *Journal of the Royal Statistical Society: Series B (Methodological)*, *57*(1), 289–300. https://doi.org/10.1111/J.2517-6161.1995.TB02031.X

Bolger, A. M., Lohse, M., & Usadel, B. (2014). Trimmomatic: A flexible trimmer for Illumina sequence data. *Bioinformatics*, *30*(15), 2114–2120. https://doi.org/10.1093/bioinformatics/btu170

Boller, T., & Felix, G. (2009). A Renaissance of Elicitors: Perception of Microbe-Associated Molecular Patterns and Danger Signals by Pattern-Recognition Receptors. *Annual Review of Plant Biology*, *60*(1), 379–406. https://doi.org/10.1146/annurev.arplant.57.032905.105346

Caño-Delgado, A., Penfield, S., Smith, C., Catley, M., & Bevan, M. (2003). Reduced cellulose synthesis invokes lignification and defense responses in Arabidopsis thaliana. *Plant Journal*, *34*(3), 351–362. https://doi.org/10.1046/j.1365-313X.2003.01729.x

Cosgrove, D. J. (2005). Growth of the plant cell wall. *Nature Reviews Molecular Cell Biology 2005 6:11*, *6*(11), 850–861. https://doi.org/10.1038/nrm1746

de Lamo, F. J., & Takken, F. L. W. (2020). Biocontrol by Fusarium oxysporum Using Endophyte-Mediated Resistance. *Frontiers in Plant Science*, *11*, 500488. https://doi.org/10.3389/FPLS.2020.00037/BIBTEX

Deacon, J. W. (1973). Phialophora radicicola and Gaeumannomyces graminis on roots of grasses and cereals. *Transactions of the British Mycological Society*, *61*(3), 471–485. https://doi.org/10.1016/s0007-1536(73)80117-2

Deacon, J. W. (1976). Biological control of the take-all fungus, Gaeumannomyces graminis, by Phialophora radicicola and similar fungi. *Soil Biology and Biochemistry*, *8*(4), 275–283. https://doi.org/10.1016/0038-0717(76)90057-2

Delgado-Baquerizo, M., Guerra, C. A., Cano-Díaz, C., Egidi, E., Wang, J. T., Eisenhauer, N., Singh, B. K., & Maestre, F. T. (2020). The proportion of soil-borne pathogens increases with warming at the global scale. *Nature Climate Change*, *10*(6), 550–554. https://doi.org/10.1038/s41558-020-0759-3

Dufresne, M., & Osbourn, A. E. (2001). Definition of Tissue-Specific and General Requirements for Plant Infection in a Phytopathogenic Fungus. *Molecular Plant-Microbe Interactions*, *14*(3), 300–307. https://doi.org/10.1094/MPMI.2001.14.3.300

Ellis, C., Karafyllidis, I., & Turner, J. G. (2002). Constitutive activation of jasmonate signaling in an Arabidopsis mutant correlates with enhanced resistance to Erysiphe cichoracearum, Pseudomonas syringae, and Myzus persicae. *Molecular Plant-Microbe Interactions*, *15*(10), 1025–1030. https://doi.org/10.1094/MPMI.2002.15.10.1025

Freeman, J., & Ward, E. (2004). Gaeumannomyces graminis, the take-all fungus and its relatives. *Molecular Plant Pathology*, *5*(4), 235–252. https://doi.org/10.1111/j.1364-3703.2004.00226.x

Freeman, J., Ward, E., Gutteridge, R. J., & Bateman, G. L. (2005). Methods for studying population structure, including sensitivity to the fungicide silthiofam, of the cereal take-all fungus, Gaeumannomyces graminis var. tritici. *Plant Pathology*, *54*(5), 686–698. https://doi.org/10.1111/j.1365-3059.2005.01252.x

Gazengel, K., Lebreton, L., Lapalu, N., Amselem, J., Guillerm-Erckelboudt, A. Y., Tagu, D., & Daval, S. (2020). pH effect on strain-specific transcriptomes of the take-all fungus. PLoS ONE, 15(7 July). https://doi.org/10.1371/journal.pone.0236429

Harris, J. M., Balint-Kurti, P., Bede, J. C., Day, B., Gold, S., Goss, E. M., Grenville-Briggs, L. J., Jones, K. M., Wang, A., Wang, Y., Mitra, R. M., Sohn, K. H., & Alvarez, M. E. (2020). What are the top 10 unanswered questions in molecular plant-microbe interactions? In *Molecular Plant-Microbe Interactions* (Vol. 33, Issue 12, pp. 1354–1365). American Phytopathological Society. https://doi.org/10.1094/MPMI-08-20-0229-CR

Henry Christopher, J. van R., & Van den Ende, W. (2018). UDP-glucose: A potential signaling molecule in plants? *Frontiers in Plant Science*, *8*, 2230. https://doi.org/10.3389/FPLS.2017.02230/BIBTEX

Hernández-Blanco, C., Feng, D. X., Hu, J., Sánchez-Vallet, A., Deslandes, L., Llorente, F., Berrocal-Lobo, M., Keller, H., Barlet, X., Sánchez-Rodríguez, C., Anderson, L. K., Somerville, S., Marco, Y., & Molinaa, A. (2007). Impairment of cellulose synthases required for Arabidopsis secondary cell wall formation enhances disease resistance. *Plant Cell*, *19*(3), 890–903. https://doi.org/10.1105/tpc.106.048058

Hernández-Restrepo, M., Groenewald, J. Z., Elliott, M. L., Canning, G., McMillan, V. E., & Crous, P. W. (2016). Take-all or nothing. *Studies in Mycology*, *83*, 19–48. https://doi.org/10.1016/j.simyco.2016.06.002

Holden, J. (1976). Infection of wheat seminal roots by varieties of Phialophora radicicola and Gaeumannomyces graminis. *Soil Biology and Biochemistry*, *8*(2), 109–119. https://doi.org/10.1016/0038-0717(76)90074-2

Huang, L., Kang, Z., & Buchenauer, H. (2001). Comparison of infection of wheat roots by Phialophora graminicola and Gaeumannomyces graminis var. tritici by ultrastructural and cytochemical studies. *Journal of Plant Diseases and Protection*, *108*(6), 593–607.

Jones, J. D. G., & Dangl, J. L. (2006). The plant immune system. *Nature*, *444*(7117), 323–329. https://doi.org/10.1038/nature05286

Kang, X., Guo, Y., Leng, S., Xiao, L., Wang, L., Xue, Y., & Liu, C. (2019). Comparative Transcriptome Profiling of Gaeumannomyces graminis var. tritici in Wheat Roots in the Absence and Presence of Biocontrol Bacillus velezensis CC09. Frontiers in Microbiology, 10(1474). https://doi.org/10.3389/fmicb.2019.01474

Kang, X., Wang, L., Guo, Y., Zain Ul Arifeen, M., Cai, X., Xue, Y., Bu, Y., Wang, G., & Liu, C. (2019). A Comparative Transcriptomic and Proteomic Analysis of Hexaploid Wheat's Responses to Colonization by Bacillus velezensis and Gaeumannomyces graminis, Both Separately and Combined. Molecular Plant-Microbe Interactions, 32(10). https://doi.org/10.1094/MPMI-03-19-0066-R

Keenan, S., Cromey, M. G., Harrow, S. A., Bithell, S. L., Butler, R. C., Beard, S. S., & Pitman, A. R. (2015). Quantitative PCR to detect Gaeumannomyces graminis var. tritici in symptomatic and non-symptomatic wheat roots. *Australasian Plant Pathology*, *44*(6), 591–597. https://doi.org/10.1007/s13313-015-0379-y

Kim, D., Paggi, J. M., Park, C., Bennett, C., & Salzberg, S. L. (2019). Graph-based genome alignment and genotyping with HISAT2 and HISAT-genotype. *Nature Biotechnology*, *37*(8), 907–915. https://doi.org/10.1038/s41587-019-0201-4

Knapp, D. G., Németh, J. B., Barry, K., Hainaut, M., Henrissat, B., Johnson, J., Kuo, A., Lim, J. H. P., Lipzen, A., Nolan, M., Ohm, R. A., Tamás, L., Grigoriev, I. V., Spatafora, J. W., Nagy, L. G., & Kovács, G. M. (2018). Comparative genomics provides insights into the lifestyle and reveals functional heterogeneity of dark septate endophytic fungi. *Scientific Reports*, *8*(1), 1–13. https://doi.org/10.1038/s41598-018-24686-4

Lee, W.-S., Rudd, J. J., Hammond-Kosack, K. E., & Kanyuka, K. (2014). Mycosphaerella graminicola LysM Effector-Mediated Stealth Pathogenesis Subverts Recognition Through Both CERK1 and CEBiP Homologues in Wheat. *C*, *27*(3), 236–243. https://doi.org/10.1094/MPMI-07-13-0201-R

Liao, Y., Smyth, G. K., & Shi, W. (2014). FeatureCounts: An efficient general purpose program for assigning sequence reads to genomic features. *Bioinformatics*, *30*(7), 923–930. https://doi.org/10.1093/bioinformatics/btt656

Livak, K. J., & Schmittgen, T. D. (2001). Analysis of Relative Gene Expression Data Using Real-Time Quantitative PCR and the 2−ΔΔCT Method. *Methods*, *25*(4), 402–408. https://doi.org/10.1006/METH.2001.1262

Lorenzo, O., Piqueras, R., Sánchez-Serrano, J. J., & Solano, R. (2003). ETHYLENE RESPONSE FACTOR1 Integrates Signals from Ethylene and Jasmonate Pathways in Plant Defense. *The Plant Cell*, *15*(1), 165–178. https://doi.org/10.1105/TPC.007468

Love, M. I., Huber, W., & Anders, S. (2014). Moderated estimation of fold change and dispersion for RNA-seq data with DESeq2. *Genome Biology*, *15*(12), 550. https://doi.org/10.1186/s13059-014-0550-8

Marcel, S., Paszkowski, U., Sawers, R., Oakeley, E., & Angliker, H. (2010). Tissue-adapted invasion strategies of the rice blast fungus Magnaporthe oryzae. *Plant Cell*, *22*(9), 3177–3187. https://doi.org/10.1105/tpc.110.078048

McMillan, V. E., Hammond-Kosack, K. E., & Gutteridge, R. J. (2011). Evidence that wheat cultivars differ in their ability to build up inoculum of the take-all fungus, Gaeumannomyces graminis var. tritici, under a first wheat crop. *Plant Pathology*. https://doi.org/10.1111/j.1365-3059.2010.02375.x

Menna, A., Dora, S., Sancho-Andrés, G., Kashyap, A., Meena, M. K., Sklodowski, K., Gasperini, D., Coll, N. S., & Sánchez-Rodríguez, C. (2021). A primary cell wall cellulose-dependent defense mechanism against vascular pathogens revealed by time-resolved dual transcriptomics. *BMC Biology*, *19*(1), 1–20. https://doi.org/10.1186/s12915-021-01100-6

Miedes, E., Vanholme, R., Boerjan, W., & Molina, A. (2014). The role of the secondary cell wall in plant resistance to pathogens. *Frontiers in Plant Science*, *5*(358). https://doi.org/10.3389/fpls.2014.00358

Nguyen, T. N., Son, S. H., Jordan, M. C., Levin, D. B., & Ayele, B. T. (2016). Lignin biosynthesis in wheat (Triticum aestivum L.): Its response to waterlogging and association with hormonal levels. *BMC Plant Biology*, *16*(1). https://doi.org/10.1186/s12870-016-0717-4

Okagaki, L. H., Nunes, C. C., Sailsbery, J., Clay, B., Brown, D., John, T., Oh, Y., Young, N., Fitzgerald, M., Haas, B. J., Zeng, Q., Young, S., Adiconis, X., Fan, L., Levin, J. Z., Mitchell, T. K., Okubara, P. A., Farman, M. L., Kohn, L. M., … Dean, R. A. (2015). *Genome Sequences of Three Phytopathogenic Species of the Magnaporthaceae Family of Fungi*. https://doi.org/10.1534/g3.115.020057

Osborne, S. J., McMillan, V. E., White, R., & Hammond-Kosack, K. E. (2018). Elite UK winter wheat cultivars differ in their ability to support the colonization of beneficial root-infecting fungi. *Journal of Experimental Botany*, *69*(12), 3103–3115. https://doi.org/10.1093/jxb/ery136

Palma-Guerrero, J., Chancellor, T., Spong, J., Canning, G., Hammond, J., McMillan, V. E., & Hammond-Kosack, K. E. (2021). Take-All Disease: New Insights into an Important Wheat Root Pathogen. *Trends in Plant Science*, *26*(8), 836–848. https://doi.org/10.1016/j.tplants.2021.02.009

Pok, B., Ngou, M., Ding, P., & Jones, J. D. G. (2022). Thirty years of resistance: Zig-zag through the plant immune system. *The Plant Cell*. https://doi.org/10.1093/PLCELL/KOAC041

Reynolds, E. S. (1963). The use of lead citrate at high pH as an electron-opaque stain in electron microscopy. *The Journal of Cell Biology*, *17*(1), 208. https://doi.org/10.1083/JCB.17.1.208

Singh, P., & Mukhopadhyay, K. (2021). Comprehensive molecular dissection of TIFY Transcription factors reveal their dynamic responses to biotic and abiotic stress in wheat (Triticum aestivum L.). *Scientific Reports*, *11*(1), 1–17. https://doi.org/10.1038/s41598-021-87722-w

Speakman, J. B., & Lewis, B. G. (1978). Limitation of Gaeumannomyces graminis by wheat root responses to Phialophora radicicola. *New Phytologist*, *80*(2), 373–380. https://doi.org/10.1111/j.1469-8137.1978.tb01571.x

Su, Z. Z., Mao, L. J., Li, N., Feng, X. X., Yuan, Z. L., Wang, L. W., Lin, F. C., & Zhang, C. L. (2013). Evidence for Biotrophic Lifestyle and Biocontrol Potential of Dark Septate Endophyte Harpophora oryzae to Rice Blast Disease. *PLOS ONE*, *8*(4), 61332. https://doi.org/10.1371/JOURNAL.PONE.0061332

Thoms, D., Liang, Y., & Haney, C. H. (2021). Maintaining symbiotic homeostasis: How do plants engage with beneficial microorganisms while at the same time restricting pathogens? In *Molecular Plant-Microbe Interactions* (Vol. 34, Issue 5, pp. 462–469). American Phytopathological Society. https://doi.org/10.1094/MPMI-11-20-0318-FI

Ulrich, K., Augustin, C., & Werner, A. (2000). Identification and characterization of a new group of root-colonizing fungi within the Gaeumannomyces-Phialophora complex. *New Phytologist*, *145*(1), 127–135. https://doi.org/10.1046/j.1469-8137.2000.00553.x

Ward, E., & Bateman, G. L. (1999). Comparison of Gaeumannomyces- and Phialophora-like fungal pathogens from maize and other plants using DNA methods. *New Phytologist*, *141*(2), 323–331. https://doi.org/10.1046/j.1469-8137.1999.00346.x

Wong, P. T. W., Mead, J. A., & Holley, M. P. (1996). Enhanced field control of wheat take-all using cold tolerant isolates of Gaeumannomyces graminis var. graminis and Phialophora sp. (lobed hyphopodia). *Plant Pathology*, *45*(2), 285–293. https://doi.org/10.1046/j.1365-3059.1996.d01-132.x

Wong, P. T. W., & Southwell, R. J. (1980). Field control of take-all of wheat by avirulent fungi. *Annals of Applied Biology*, *94*(1), 41–49. https://doi.org/10.1111/j.1744-7348.1980.tb03894.x

Yang, L., Xie, L., Xue, B., Goodwin, P. H., Quan, X., Zheng, C., Liu, T., Lei, Z., Yang, X., Chao, Y., & Wu, C. (2015). Comparative Transcriptome Profiling of the Early Infection of Wheat Roots by Gaeumannomyces graminis var. tritici. PLOS ONE, 10(4), e0120691. https://doi.org/10.1371/journal.pone.0120691

Zaninotto, F., Camera, S. La, Polverari, A., & Delledonne, M. (2006). Cross Talk between Reactive Nitrogen and Oxygen Species during the Hypersensitive Disease Resistance Response. *Plant Physiology*, *141*(2), 379–383. https://doi.org/10.1104/PP.106.078857

Zhang, Y., Xu, K., Yu, D., Liu, Z., Peng, C., Li, X., Zhang, J., Dong, Y., Zhang, Y., Tian, P., Guo, T., & Li, C. (2019). The highly conserved barley powdery mildew effector BEC1019 confers susceptibility to biotrophic and necrotrophic pathogens in wheat. *International Journal of Molecular Sciences*, *20*(18), 1–16. https://doi.org/10.3390/ijms20184376

Zhang, J., Yan, H., Xia, M., Han, X., Xie, L., Goodwin, P. H., Quan, X., Sun, R., Wu, C., & Yang, L. (2020). Wheat root transcriptional responses against Gaeumannomyces graminis var . tritici. Phytopathology Research, 2(23). https://doi.org/https://doi.org/10.1186/s42483-020-00066-7

Zhou, F., Emonet, A., Dénervaud Tendon, V., Marhavy, P., Wu, D., Lahaye, T., & Geldner, N. (2020). Co-incidence of Damage and Microbial Patterns Controls Localized Immune Responses in Roots. *Cell*, *180*(3), 440–453. https://doi.org/10.1016/j.cell.2020.01.013

Zhu, T., Wang, L., Rimbert, H., Rodriguez, J. C., Deal, K. R., De Oliveira, R., Choulet, F., Keeble-Gagnère, G., Tibbits, J., Rogers, J., Eversole, K., Appels, R., Gu, Y. Q., Mascher, M., Dvorak, J., & Luo, M. C. (2021). Optical maps refine the bread wheat Triticum aestivum cv. Chinese Spring genome assembly. *The Plant Journal*, *107*(1), 303–314. https://doi.org/10.1111/TPJ.15289